Design and control of patterns in reaction-diffusion systems

Vladimir K. Vanag and Irving R. Epstein
Department of Chemistry and Volen Center for Complex Systems, Brandeis University, Waltham, Massachusetts 02454-9110, USA

(Received 10 January 2008; accepted 26 February 2008; published online 27 June 2008)

We discuss the design of reaction-diffusion systems that display a variety of spatiotemporal patterns. We also consider how these patterns may be controlled by external perturbation, typically using photochemistry or temperature. Systems treated include the Belousov–Zhabotinsky (BZ) reaction, the chlorite-iodide-malonic acid and chlorine dioxide-malonic acid-iodine reactions, and the BZ–AOT system, i.e., the BZ reaction in a water-in-oil reverse microemulsion stabilized by the surfactant sodium bis(2-ethylhexyl) sulfosuccinate (AOT). © *2008 American Institute of Physics*. [DOI: 10.1063/1.2900555]

The initial instances of phenomena such as chemical oscillation, traveling waves, and Turing patterns in chemically reactive media were discovered by serendipity. Once one gains an understanding of the underlying dynamics of such phenomena, even at a relatively crude level, it becomes feasible to design new systems that exhibit these behaviors and to control the patterns they display. We discuss here some approaches to generating selected spatiotemporal behaviors in reaction-diffusion systems and then look at how external influences, particularly light and temperature, may be employed to control these patterns.

I. INTRODUCTION

From the initial discoveries of the Bray[1] and Belousov–Zhabotinsky (BZ)[2,3] oscillating reactions to the first experimental demonstration of Turing patterns,[4] the history of nonlinear chemical dynamics is replete with examples of serendipitous discovery. Much of the development of the field can be viewed as an evolution from accidental discovery of a phenomenon to theoretical analysis leading to methods for deliberate design and even control. The statement by one investigator about dynamic phenomena in social systems, "If you didn't build it, you didn't explain it,"[5] pertains equally to reaction-diffusion systems.

Probably the first successful examples of this principle applied to chemical systems were the efforts of the Brandeis group in the early 1980s[6] to build the first deliberately designed chemical oscillators. Working from a simple mathematical model, the "cross-shaped phase diagram," developed by Boissonade and De Kepper,[7] that stressed the importance of autocatalysis, open systems, bistability, and slow negative feedback, these investigators found inorganic chemical reactions possessing kinetics that fulfilled the conditions of the model. After their initial success with the arsenite-iodate-chlorite system, they and others were able to use the design algorithm to construct literally dozens of new chemical oscillators and even to develop a taxonomy of oscillator families.[8] Guided by a model of a biochemical system,[9] the same group later coupled the chlorite-iodide[10] and bromate-iodide[11] oscillators to build a system exhibiting birhythmicity, or bistability between two different modes of oscillation, the bromate-chlorite-iodide reaction.[12]

Our focus here is on spatial and spatio-temporal pattern formation rather than on the simpler temporal patterning described above. Nevertheless, the process is similar: insight into the key feature(s) of the phenomenon leads to design of an algorithm, often based on an oversimplified mathematical model, which makes it possible to design systems that display a phenomenon first discovered serendipitously. In addition to describing efforts to design systems that exhibit particular forms of spatial pattern formation, we also discuss the related issue of controlling patterns, i.e., of choosing conditions that force a system to display a desired type of pattern. Rather than attempting to provide a comprehensive review of the entire field, we focus on some of our own results, complemented where appropriate by the work of others.

II. EARLY PATTERNS: THE CIMA SYSTEM AND THE CFUR

The first spatial patterns to be studied in nonlinear dynamics were the targets and spirals found in the BZ reaction.[13,14] These fascinating structures are of considerable interest not only in chemistry, but in biology as well, where very similar structures are seen in such phenomena as aggregating slime molds[15,16] and calcium waves in fertilized oocytes.[17,18] Although the cross-shaped phase diagram approach yielded a wide variety of novel oscillators, many based on the versatile chemistry of the chlorite ion,[19,20] none proved capable of producing the sort of spatial patterns found in the unstirred BZ system. The reason was clear: these reactions oscillated only in a flow reactor, where the reactants were continuously replenished, while the BZ oscillator could function in a closed (batch) configuration for an hour or more. To build other systems that showed spatial patterns like the BZ, one needed to do one of two things: either make a new batch oscillator or design a reactor that allowed for the influx of fresh reactants without stirring the reaction mixture.

 © 2008 American Institute of Physics

Downloaded 27 Jun 2008 to 129.64.51.176. Redistribution subject to AIP license or copyright; see http://chaos.aip.org/chaos/copyright.jsp

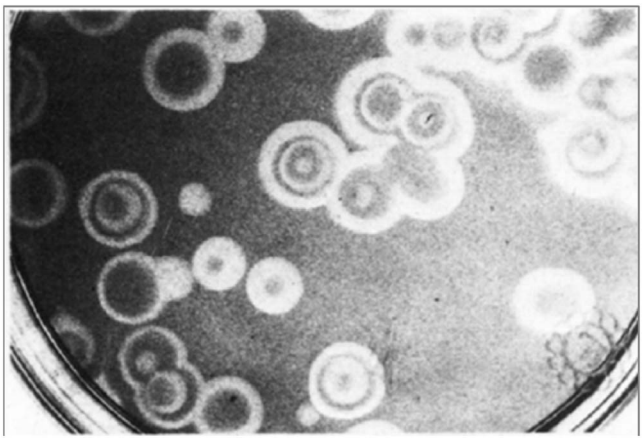

FIG. 1. Trigger wave pattern observed at 5.0 °C in a 2 mm layer of aqueous solution with initial composition $[CH_2(COOH)_2]=0.0033$ M; [NaI] $=0.09$ M; $[NaClO_2]=0.1$ M; $[H_2SO_4]=0.0056$ M, and starch as an indicator (Ref. 21).

Both solutions to the problem were ultimately implemented, and both led to the discovery of additional pattern formation phenomena. The first breakthrough, carried out in a deliberate effort to generate new pattern-forming systems, was the development of the chlorite-iodide-malonic acid (CIMA) batch oscillator.[21] Figure 1 shows target patterns observed in this reaction. While it gives less robust and shorter-lived patterns than the BZ reaction, the CIMA system, as we shall see later, has come to play a major role in the development of nonlinear chemical dynamics in both the design and the control of spatial patterns.

The alternative approach of running a reaction in an unstirred configuration that allowed an inflow of fresh reactants (and an outflow of reacted material) was adopted by the Austin group, who succeeded in designing the first continuously fed unstirred reactors (CFURs) shown in Fig. 2.[22] Utilizing either a gel[22] or a porous glass[23] as the reaction medium, these researchers were able to generate and sustain patterns for periods of time significantly longer that those possible in experiments conducted in a closed petri dish. This capability made it possible to utilize reactions like the ferrocyanide-iodate-sulfite (FIS) reaction,[24] which can oscillate only in an open system. The FIS reaction turns out to exhibit a rich variety of new spatiotemporal patterns such as breathing spots[25] and spot splitting.[26]

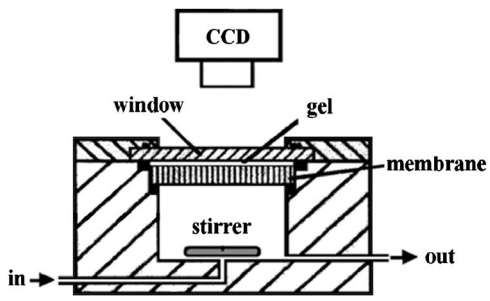

FIG. 2. Design of a CFUR. Reaction takes place in the thin layer of gel, which exchanges chemicals through the membrane with the continuous flow stirred tank reactor (CSTR) below it. Patterns are monitored with the CCD camera (Ref. 22).

III. DESIGNING TURING PATTERNS

Among the most challenging patterns to construct have been the spatially periodic, temporally stationary patterns suggested by Turing[27] in 1952 as a possible origin for morphogenesis in living organisms. The major difficulty is that the existence of Turing patterns requires that two species in the system, the activator and the inhibitor, diffuse at very different rates, with diffusion coefficients separated by about an order of magnitude. Since small molecules in aqueous solution all have diffusion coefficients within about a factor of 2 of 2×10^{-5} cm^2 s^{-1}, simple reaction-diffusion systems did not lend themselves to generating Turing patterns. Of course, biological systems contain macromolecules with a wide range of sizes and hence diffusion coefficients. It proved difficult, however, to identify unambiguously the actual activator and inhibitor in any candidate system.[28,29]

Four decades after Turing's theoretical work, the Bordeaux group produced the first experimental demonstration of the Turing phenomenon.[4] The experiments were carried out in a gel CFUR in a search for patterns in the CIMA reaction, but the emergence of Turing patterns was unanticipated. Analysis of the Bordeaux experiments[30] revealed that, by using starch as an indicator in their gel, Castets *et al.* had serendipitously generated the necessary difference in diffusion rates between the activator, iodide, and the inhibitor, chlorite. Although both of these free species diffuse at similar rates through the gel, which is mostly water, starch molecules are significantly larger and are essentially trapped and immobilized within the pores of the gel. Iodide, the activator, forms a reversible complex with starch and iodine, an intermediate produced in the reaction. Thus, the diffusion of iodide (and iodine) through the starch impregnated gel resembles a random walk through a region containing randomly spaced traps, which the walker intermittently falls into and climbs out of. The net result is a slowing of the diffusion of the activator species by about an order of magnitude, just what is needed to generate Turing patterns!

Lengyel and Epstein exploited this insight and their further studies of the mechanism of the CIMA reaction, first to construct a more robust version of the system, the chlorine dioxide-iodine-malonic acid (CDIMA) reaction,[31] and then to propose a general algorithm for designing systems that display Turing patterns.[32] Their approach starts from a generic two variable activator-inhibitor model and shows that if the activator can form an immobile, reversible complex with a third species, then one can tune the concentration of this complexing agent to effectively renormalize the diffusion coefficients in a way that makes it possible for Turing patterns to arise.

IV. ANOTHER APPROACH: THE BZ–AOT SYSTEM

An alternative route to generating the difference in diffusion coefficients needed to produce Turing patterns is to employ a microheterogeneous medium, e.g., a microemulsion, where the structure of the medium results in different species diffusing at very different rates, even in the absence of chemical reaction. A water-in-oil, or reverse, microemulsion consists of nanodroplets of water, each surrounded by a

Downloaded 27 Jun 2008 to 129.64.51.176. Redistribution subject to AIP license or copyright; see http://chaos.aip.org/chaos/copyright.jsp

shell of surfactant molecules and residing in the continuous oil phase, where they diffuse with diffusion coefficient $D_d = (10^{-6}-10^{-7})$ cm^2 s^{-1}, depending on the radius of the droplets. If the system contains both hydrophobic and hydrophilic solutes, small oil-soluble molecules diffuse through the oil phase at typical molecular rates ($D_m \sim 2\times 10^{-5}$ cm^2 s^{-1}). Water-soluble species, on the other hand, reside in the tiny droplets, within which diffusion is irrelevant, since a typical droplet diameter ($\cong$10 nm) is much less than one diffusion length, given by $(\tau D_m)^{1/2} \cong 10^5$ nm at a typical reaction time of $\tau = 10$ s. Instead, these molecules diffuse with entire droplets, at rates D_d, one to two orders of magnitude slower than the diffusion of the oil-soluble species.

In the BZ reaction, all reactants are water soluble, but two intermediates of the reaction, Br_2 and $BrO_2^{\cdot}$, are oil soluble and can diffuse much more rapidly than the reactants. The radical $BrO_2^{\cdot}$ serves as an activator, while Br_2 plays the role of a fast diffusing inhibitor. The well-studied aerosol OT (AOT) water-in-oil microemulsion[33] turns out to be an excellent medium in which to probe the BZ reaction. Many patterns, some of them never before observed, have been found in the BZ–AOT system. Transitions between patterns can be induced by changing the initial concentrations of reactants or by modifying the physical structure of the AOT microemulsion. For example, the average radius R_w of water nanodroplets depends on the ratio $\omega = [H_2O]/[AOT]$ approximately as $R_w/\text{nm} \cong 0.17\omega$.[34–36] Alternatively, one may vary the spacing between droplets by changing the ratio of water to oil at constant ω, i.e., the volume droplet fraction φ_d. The temperature affects not only the reaction rates but also the diffusion coefficients and the proximity of the AOT microemulsion to the percolation transition, which occurs at a critical value of φ_d. Turing patterns, as well as many other patterns, some of which we discuss below, have been found in this very rich system.

V. CONTROLLING PATTERNS

The basic idea in controlling spatiotemporal patterns in reaction-diffusion systems is that, if one understands the underlying dynamics, one can force the system to display a desired pattern by imposing a relatively weak external perturbation. Conceptually, this approach is closely related to the design algorithms described above. Typically, the control is accomplished by externally forcing a control parameter that affects the concentrations of the chemical species. For example, for photosensitive systems one might vary the intensity or the frequency of imposed illumination. Temperature is a promising control parameter, since it affects both reaction rates and transport properties. In the following discussion, we focus as much as possible on examples of controlling patterns in excitable and oscillatory systems that differ from those described in the excellent review by Mikhailov and Showalter.[37]

Nonlinear systems often give rise to multistability, i.e., the existence of two or more stable states, which may be stationary or dynamic, e.g., oscillatory or chaotic, under the same set of parameters.[38] In spatially extended nonlinear systems this phenomenon is even more common than in point or well-stirred systems, and experiments[39] and models[40] show tri- and even tetrastability. In a multistable system, the final state attained by the system depends on the initial conditions or, equivalently, on the prehistory of the system. Therefore, one can utilize the initial conditions as a sort of control parameter. For spatially extended systems, we can also employ the boundary conditions to control pattern selection.

A. Control by initial conditions

Turing patterns generally occur in one of three forms: hexagonal spots, stripes (or labyrinthine patterns), and honeycombs (or reversed hexagons). Coexistence of hexagons and stripes or of stripes and honeycombs can be found at the same parameters,[41] e.g., in experiments on the CIMA system[42] and in the LE model[30] for the CDIMA reaction.[21,43]

In Fig. 3, we show examples of stationary Turing patterns belonging to the class of superlattices, i.e., patterns that have at least two different characteristic wavelengths, in the spatially extended photosensitive CDIMA reaction.[44] The rightmost column contains the final patterns that evolve after brief illumination of the initial labyrinthine patterns through the masks shown in the left column. After this initial illumination, the masks and the light source are removed, and the Turing patterns then develop in the dark. In the upper row, the pattern that emerges is a so-called "black eye" pattern, first found serendipitously in a two-sided CFUR.[45] In the middle row, the pattern resembles the "white eye" patterns, also found initially by chance, in experiments with two interacting gel layers.[44] The bottom row of Fig. 3, where the ratio between the characteristic sizes of the mask and the native labyrinthine Turing patterns is equal to 4, exhibits the emergence of even more complex, higher order patterns.

In Fig. 4, we demonstrate an example of photochemical control of localized patterns, where the observed behavior depends not only on the initial configuration, i.e., the shape

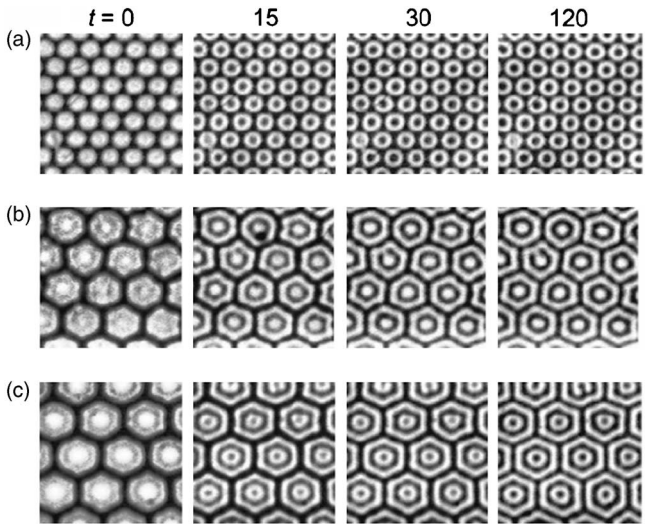

FIG. 3. Stationary Turing patterns in the CDIMA reaction developed after illumination through a mask. The ratio between the characteristic wavelengths of the mask and the native Turing patterns is equal to 2, 3, and 4, respectively, for rows (a), (b), and (c). The numbers above the columns show the time (in min) after cessation of illumination. Frame size $=5\times 5$ mm^2 (Ref. 44).

Downloaded 27 Jun 2008 to 129.64.51.176. Redistribution subject to AIP license or copyright; see http://chaos.aip.org/chaos/copyright.jsp

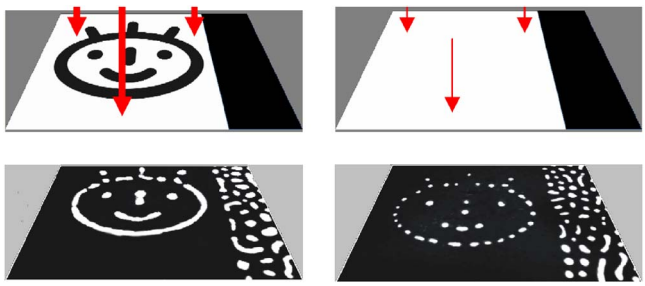

FIG. 4. (Color online) Pattern memory utilizing localized spots in the BZ–AOT system. (Left column) illumination of the BZ–AOT reaction through a "face-mask" for 5 min at intensity $I=I_0$ sufficient to suppress all patterns. Right part of the reactor (narrow stripe with Turing stationary spots) remains in darkness. $I_0=28$ mW/cm^2. (Right column) subsequent illumination without any mask for 1 h at intensity $I=I_0/5$. This intensity of light prevents the emergence of new spots, but cannot suppress already existing patterns. Size of snapshots is 7.7 mm$\times$5.8 mm. $[\text{malonic acid}]_0=0.1$ M, $[H_2SO_4]_0=0.3$ M, $[NaBrO_3]_0=0.25$ M, $[Ru(bpy)_3]_0=0.004$ M; volume fraction of aqueous droplets $\varphi_d=0.45$, $\omega\equiv[H_2O]/[AOT]=10$ (Ref. 46).

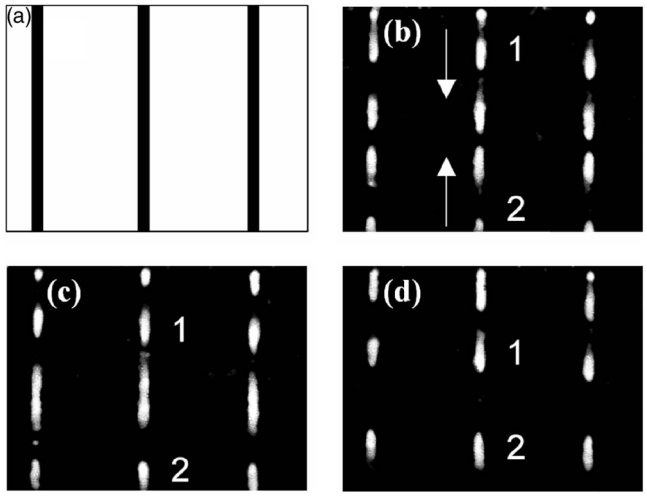

FIG. 5. Localized waves in the BZ–AOT system (a) mask. Time interval between snapshots (b) and (c) is 30 s and between snapshots (c) and (d) is 36 s. Numbers 1 and 2 mark two approaching waves. The width of the waves is ~0.18 mm. The period is 150 s. $\omega\equiv[H_2O]/[AOT]=12$, $\varphi_d=0.35$, $[H_2SO_4]=0.27$ M, $[NaBrO_3]=0.3$ M, $[MA]=0.1$ M, $[Ru(bpy)_3^{2+}]=3.6$ mM. Vertical size=5 mm (Ref. 111).

of the mask, but also on the intensity of the light. In the photosensitive $Ru(bpy)_3$-catalyzed BZ–AOT system, it is possible to tune the intensity of homogeneous illumination in such a way that the system lies close to the onset of Turing instability. Under these conditions, the BZ–AOT system displays hysteresis and bistability between a homogeneous steady state and stationary Turing or localized patterns.[46] In the dark, Turing patterns form spontaneously. If the light intensity, I, is slowly increased, the patterns initially change only slightly, but at a critical intensity, I_{sc}, they suddenly vanish, and the homogeneous steady state (SS) is seen. If we then slowly decrease I, the Turing patterns spontaneously re-emerge at a lower intensity, I_c. For $I_c<I<I_{sc}$, the system is bistable. In this bistable range of I, localized Turing patterns generated by a local perturbation can be stable, while Turing patterns cannot emerge spontaneously elsewhere in the medium, since the SS is also stable. Since a combination of localized spots can be designed to create any image, this regime of the BZ–AOT system can be utilized for image storage.

Under slightly different conditions, the $Ru(bpy)_3$-catalyzed BZ–AOT system can generate localized waves, if a thin layer of BZ–AOT microemulsion is illuminated through a striped mask [Fig. 5(a)] for a short period of time (3–5 min).[47] After the emergence of the first wave, the mask is removed and the intensity of the now homogeneous illumination is decreased. As shown in Figs. 5(b) and 5(c), waves propagate only in the narrow stripes that had been screened by the mask. The shapes of these dark channels in Fig. 5(a) and the paths of the resulting waves can be arbitrarily chosen, so that the waves change their direction according to the shape of the mask. In this fashion, one can establish a connection or communication route between any two points in the system via traveling waves. One can imagine combining controllable images (memory) and localized waves (information traffic) in such a system to build a device capable of a crude form of chemical computation. Localized waves under global and local photocontrol have also been obtained in the aqueous BZ system.[48,49]

B. Global feedback

Another form of photochemical control of patterns in the oscillatory photosensitive $Ru(bpy)_3$-catalyzed BZ reaction can be accomplished by using global negative feedback.[50,51] The average concentration of $Ru(bpy)_3^{3+}Z_{av}$, taken over the working area of a gel reactor, is employed to control the intensity I of illumination according to $I=I_{max}\sin^2[g(Z_{av}-Z_t)]$, where g is a feedback coefficient and Z_t is a target concentration that can be arbitrarily varied electronically, but is usually set close to the steady state value, Z_{ss}. As soon as Z_{av} increases (due to autocatalysis in some small region), I also increases and can suppress autocatalysis (or oscillation) in all other areas. The effectiveness of pattern suppression depends on the light intensity I and consequently on the coefficient g. If all patterns are suppressed by light and Z_{av} becomes almost equal to Z_t, the light intensity drops to essentially zero, resulting in autocatalysis starting in a new portion of the medium due to the oscillatory nature of the system.

In such a system, the local coupling between neighboring areas due to diffusion becomes less important, and new types of patterns, such as oscillatory clusters, emerge. Such a pattern consists of two or more regions (each of which may have several spatially disjoint subregions) in each of which all the points oscillate with the same amplitude and phase. In a sense, clusters resemble standing waves,[52–54] except that clusters lack a characteristic wavelength. Depending on g, different types of oscillatory clusters can arise: standing clusters [Figs. 6(a) and 6(b)] occur at lower values of g, irregular clusters [Figs. 6(c)–6(f)] at intermediate g, and localized clusters at larger g.

The shape of a standing cluster depends on the initial conditions. For example, the clusters shown in Figs. 6(a) and 6(b) evolved from an initial spiral wave, and the average distance between two neighboring rings of the same color in the cluster pattern is approximately equal to the wavelength

Downloaded 27 Jun 2008 to 129.64.51.176. Redistribution subject to AIP license or copyright; see http://chaos.aip.org/chaos/copyright.jsp

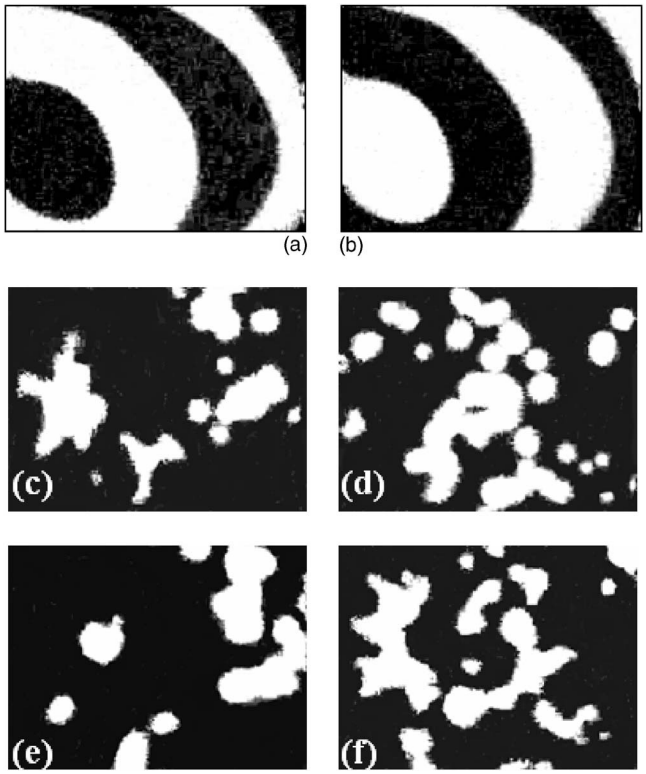

FIG. 6. (a), (b) Standing oscillatory clusters that evolve from an initial spiral wave. Time between snapshots is 18 s. $[H_2SO_4]_0=0.7$, $[BrO_3^-]_0=0.4$, $[MA]_0=0.2$, $[Br^-]_0=0.125$, $g=5.5\times10^4$. (c)–(f) Irregular oscillatory clusters. $[H_2SO_4]_0=0.75$, $[BrO_3^-]_0=0.312$, $[MA]_0=0.375$, $[Br^-]_0=0.125$; $g=1.5\times10^5$ M^{-1}. $Ru(bpy)_3^{3+}$ catalyzed BZ reaction in a silica-gel, CSTR (Ref. 50).

of the initial spiral. If stripes or circles are initially imprinted on the medium by brief illumination through a mask, the oscillatory standing clusters retain that shape, as shown in Fig. 7.

C. Periodic forcing

External periodic forcing of oscillatory systems has a long history in nonlinear dynamics. Examples of such phenomena include the interaction between two oscillators (since each oscillator can be considered as an external force exerted on the other), synchronization of a large number of oscillators, resonances, frequency locking, Arnol'd tongues, and circadian rhythms.[38] We focus here on the periodic forcing of spatially extended dynamical systems. The corresponding point system can be in an excitable or an oscillatory state as well as being subject to Turing or wave instabilities. We consider these cases separately, starting with excitable systems.

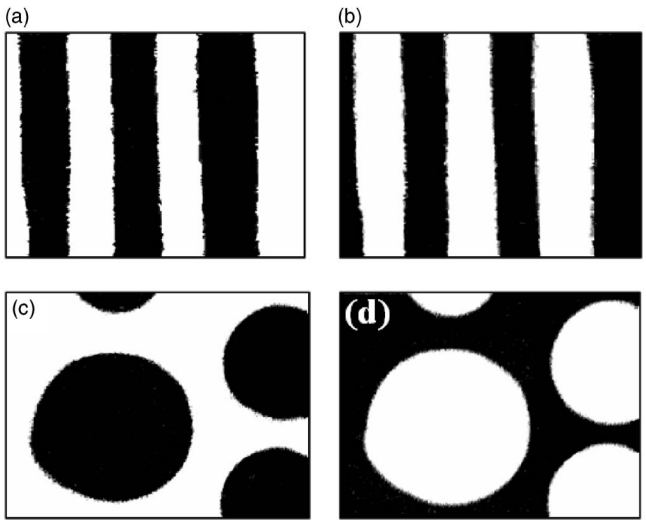

FIG. 7. Oscillatory standing clusters in the BZ reaction with negative global feedback (Ref. 51).

There is a large body of theoretical work on periodic forcing of excitable and oscillatory media,[55–69] but we focus here on some key experimental results that have led to new types of patterns. Spiral waves are the most common patterns in excitable media. The spiral tip may be either moving (meandering) or stationary (pinned), leading to two types of spirals, respectively, meandering and rigidly rotating. Agladze *et al.*[70] found that the tip of a rigidly rotating spiral wave in a thin layer of the photosensitive BZ reaction can be caused to drift, together with the entire spiral, at a constant velocity by spatially homogeneous, temporally periodic illumination at a frequency equal to that of the spiral. The shape of the spiral does not change during this drift.[71] These results were confirmed in later work,[72–74] and detailed simulations[74] gave excellent agreement between the experiments and a simple model consisting of Eqs. (1) and (2), the photosensitive Oregonator.[75] Here u and z represent the key chemical species, while I is the intensity of illumination. In Fig. 8 we compare the experiments (a) and the simulations (b). It is remarkable that so simple a model can explain such complex behavior,

$$\partial u/\partial\tau=(1/\varepsilon)[(q-u)(fz+I)/(q+u)+u-u^2]+\Delta u, \quad (1)$$

$$\partial z/\partial\tau=u-z, \quad (2)$$

where the Laplacian $\Delta=\partial^2/\partial x^2+\partial^2/\partial y^2$ in 2D, and x and y are the spatial coordinates.

For meandering spirals, resonances between the period of illumination and the intrinsic period of the spiral also exist and take the form of Arnol'd tongues, as shown in Fig. 9, calculated from the same Eqs. (1) and (2), but for parameters that correspond to meandering spirals. Again, the simulations coincide well with the experimental data. Comparing Figs. 8 and 9, we see that resonant drift of a spiral occurs for both rigid and meandering spirals, but in the latter case this resonance occurs at periods T_m significantly larger than T_0, though still in the 1:1 Arnol'd tongue.

These examples demonstrate that spiral wave behavior in excitable media can be controlled if the intensity of illumination is smaller than the critical level at which waves are suppressed. Consider now periodic illumination of the spatially extended BZ system in the oscillatory regime and at a light intensity above the critical one. Petrov *et al.*[23] found clusters by periodically illuminating the same spatially extended photosensitive BZ reaction under conditions where the point system oscillates. The dependence of the cluster type on the frequency f of illumination is shown in Fig. 10.

At $f/f_0=1$, one finds only homogeneous bulk oscillations. At $f/f_0=1.5$, the system is not able to synchronize with

Downloaded 27 Jun 2008 to 129.64.51.176. Redistribution subject to AIP license or copyright; see http://chaos.aip.org/chaos/copyright.jsp

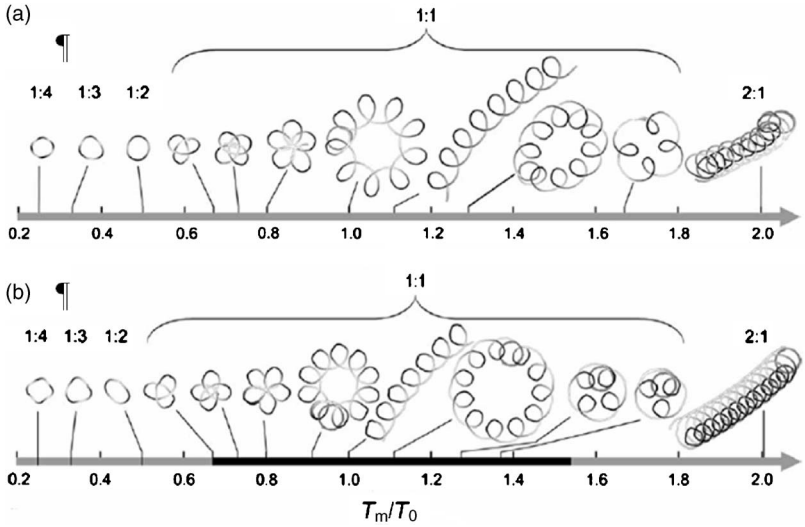

FIG. 8. Trajectories of a spiral tip under periodic sinusoidal illumination of the BZ reaction for different ratios T_m/T_0, where T_m is the modulation period and T_0 is the spiral wave period. (a) Experiment, $T_0=30.3$ s. (b) Simulations of Eqs. (1) and (2) at $\varepsilon=0.05$, $q=0.002$, $f=3.5$, and $I=I_0+A\sin(2\pi\tau/T_m)$, $I_0=0.01$, $A=0.001$. I_0 corresponds to the background constant illumination in experiments with intensity of 0.05 mW cm^{-2}. The ratio $n:m$ gives the number of lobes n per m periods of modulation (Ref. 74).

the perturbation, and randomly emerging "bubbles" are observed. At $f/f_0=2$, standing 2-phase oscillatory clusters, like those found with global negative feedback,[50] occur. Three-phase clusters, also found in experiments with global feedback, in which the phases of the three oscillatory clusters are shifted by $2\pi/3$, emerge at $f/f_0=3$. After three periods of perturbation, the original pattern is recovered.

Clearly, changing the frequency of external forcing allows one to control patterns. The frequency of perturbation is not the only parameter that determines patterning in an oscillatory medium. Varying the duration of the illuminated (T_L) and dark (T_D) periods at constant frequency can also lead to changes in the type of clusters observed.[76] In Fig. 11, clusters are found in a triangular region of the T_L-T_D plane. Along the dotted line (corresponding to $T_L+T_D=$constant), two-phase standing clusters, three-phase clusters, irregular clusters, and localized clusters are observed, though the perturbation period remains fixed. These observations are explained by the fact that different amounts of inhibitor (Br^-) are photoinjected into the system in each period, depending on the ratio T_L/T_D.

Lin *et al.*[77] demonstrated that, at fixed ratio $T_L/T_D=1$, a transition from wave patterns to standing clusters can be induced by increasing the light intensity. In Fig. 12, patterns (a) and (b) are definitely wave patterns, (c) and (d) are mixed patterns, (e) is irregular oscillatory clusters, and (f) and (g) are two-phase standing clusters. To differentiate among the types of patterns, the authors introduced a novel Fourier transform shown in the bottom row of Fig. 12. A wave pattern corresponds to a circle, while a two-phase standing cluster gives two points along a diameter connected by a straight line. Three- and four-phase clusters have also been found in the periodically illuminated BZ system.[78,79]

D. Traveling modulation

Recently, a new type of periodic forcing was introduced, so-called traveling-wave forcing or modulation.[41,80–85] Suppose we have a pattern, e.g., spiral waves,[83] Turing patterns[80,81] or even a homogeneous steady state (SS),[41] that occupies the entire medium. We impose a perturbation, e.g., illumination of a photosensitive system through a mask, in the form of a long narrow stripe. In the perturbed region, the

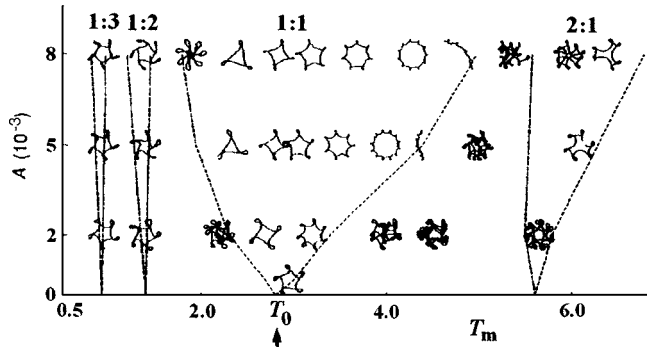

FIG. 9. Simulations of Eqs. (1) and (2). Tip trajectories in response to sinusoidal illumination with amplitude A and period T_m. Dashed lines indicate boundaries of entrainment bands for ratios $n:m$, the number of lobes per m periods of modulation. $\varepsilon=0.05$, $q=0.002$, and $f=2.0$. T_0 (marked by the arrow) is the intrinsic period of an unperturbed meandering spiral (Ref. 75).

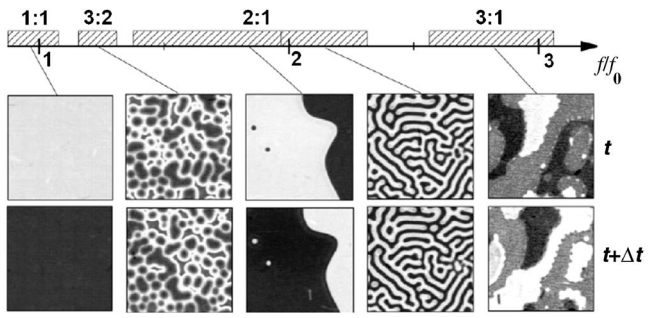

FIG. 10. Frequency-locked regimes for the periodically illuminated BZ reaction; f is the frequency of the light; f_0 is the natural frequency of bulk oscillation. Patterns in upper and bottom rows are separated in time by $\Delta t=1/f$ except for the 1:1 resonance where $\Delta t=1/(2f)$. The BZ system was illuminated for 6 s with constant light intensity for all experiments; at $f/f_0=1$ the period of forcing is 36 s, and at $f/f_0=3$ the period of forcing is 12 s (Ref. 23).

Downloaded 27 Jun 2008 to 129.64.51.176. Redistribution subject to AIP license or copyright; see http://chaos.aip.org/chaos/copyright.jsp

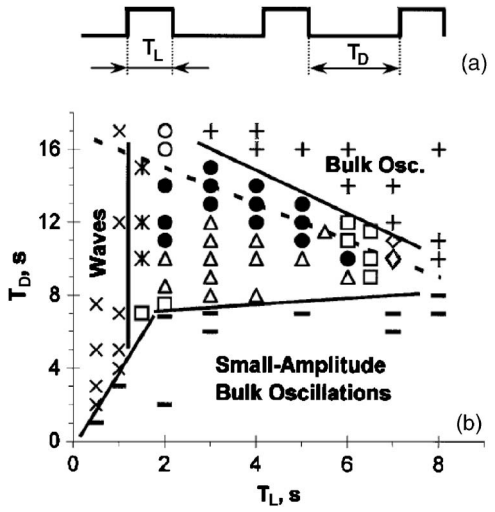

FIG. 11. (a) Shape of external light signal. During period T_L, the intensity of illumination $I_{act}=15$ mW/cm^2; during T_D, $I_{act}=0$. (b) Dependence of system behavior on T_L and T_D; symbols: (×) wave patterns, (−) small amplitude bulk oscillations, (+) high amplitude bulk oscillations, (●) two-phase standing clusters, (△) three-phase clusters, (□) irregular clusters, (◇) localized clusters, (∗) mixed behavior—clusters and waves in different parts of the gel. Along the dotted line, $T_L+T_D=T_0$. Initial reagent concentrations, 1.5 mM of immobilized $Ru(bpy)_3^{2+}$ in gel; $[H_2SO_4]_0=0.75$ M, $[NaBrO_3]_0=0.312$ M, [malonic acid]$_0=0.375$ M, $[NaBr]_0=0.125$ M in feeding chamber (Ref. 76).

illumination causes the system to switch into another state. For example, if we start from the homogeneous SS, we may have Turing patterns (spots or stripes) in the illuminated stripe. Now let us start moving the mask perpendicular to the direction of the stripe at a constant velocity. This spatiotemporal perturbation can induce new patterns, whose nature depends on the velocity and width of the mask, as well as on the type of patterns in the unperturbed and perturbed regions.

When the mask velocity is below a threshold value, the patterns in the stripe simply translate with the mask. Above the threshold, however, the patterns cannot follow, and nontranslational motion occurs.[41] This mechanism allows us to explain the "jumping waves" found recently in the BZ–AOT system at temperatures above ambient.

E. Temperature as a control parameter

The use of temperature, T, as a control parameter dates back at least to the first experiments on Turing patterns in the CIMA reaction.[4] Turing patterns were found at $T<10$ °C. Above this temperature, only wave patterns originating from bulk oscillations occur in this system. It was shown theoretically using the Brusselator[86] and extended Oregonator[87] models that interaction between Turing and Hopf (oscillatory) modes can generate a new type of pattern, an oscillatory Turing pattern. These patterns are stationary in space, but oscillatory in time. The first experimental evidence of the oscillatory Turing patterns was obtained in the BZ–AOT system,[87] also due to the interaction between Turing and Hopf instabilities. If one changes temperature or some other parameter, e.g., light intensity, in such a way that the relative contributions of the two modes changes, it may be possible to find oscillatory Turing patterns in the parameter range between pure Turing and pure wave patterns.

Such an approach was realized in the CDIMA system using light to partially suppress the oscillatory mode (see Fig. 13).[88] An analogous approach, but using temperature as the control parameter, was utilized in the BZ–AOT system.[39] In the BZ–AOT system, changing the temperature affects not the only reaction rates, but the structure of the microemulsion as well.[89–92] At low temperatures, the system is below the percolation transition, and each water droplet is isolated from the other droplets by a surfactant shell and by the continuous oil phase. As T increases, droplets first form clusters and then dynamical water channels that traverse the entire microemulsion. The diffusion coefficients of water-soluble molecules above and below the percolation transition are very different, which enhances the effect of temperature on patterns in the BZ–AOT system.

In Fig. 14 we display oscillatory Turing patterns found quite recently in the $Ru(bpy)_3$-catalyzed BZ–AOT system due to variation in temperature. At $T=25$ °C, the system exhibits stationary Turing patterns. At $T=45$ °C, we observe the familiar spiral waves, while at an intermediate temperature, $T=30$ °C, oscillatory in-phase Turing patterns are found. The space-time plot in Fig. 14(c) shows that the striped patterns shown in Fig. 14(b) oscillate in-phase. Out-

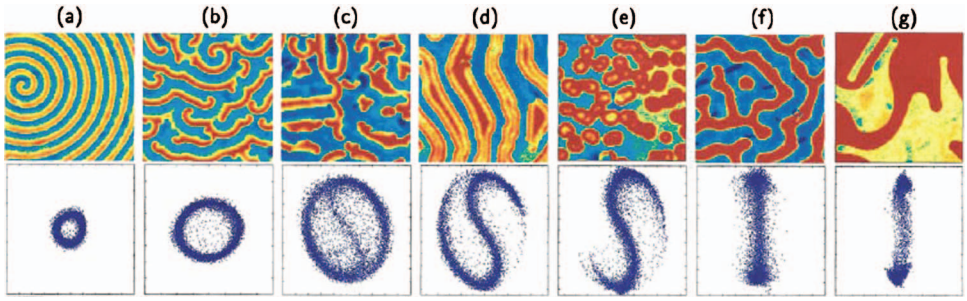

FIG. 12. (Color) (Top row) patterns in the BZ reaction (image size=9×9 mm^2, false color) at increasing light intensity I and slightly decreasing frequency f. Values of I(W/m^2) and f(Hz)=(a) 0, 0; (b) 0.1, 119; (c) 0.0625, 214; (d) 0.0556, 248; (e) 0.0417, 358; (f) 0.0455, 386; (g) 0.0385, 412. (Bottom row) the complex Fourier amplitude A for each pattern: the abscissa is Re(A) and the ordinate is Im(A). Each point in the complex plane corresponds to the temporal Fourier amplitude A of a pixel in the image after frequency demodulation at $f/2$ (Ref. 77).

Downloaded 27 Jun 2008 to 129.64.51.176. Redistribution subject to AIP license or copyright; see http://chaos.aip.org/chaos/copyright.jsp

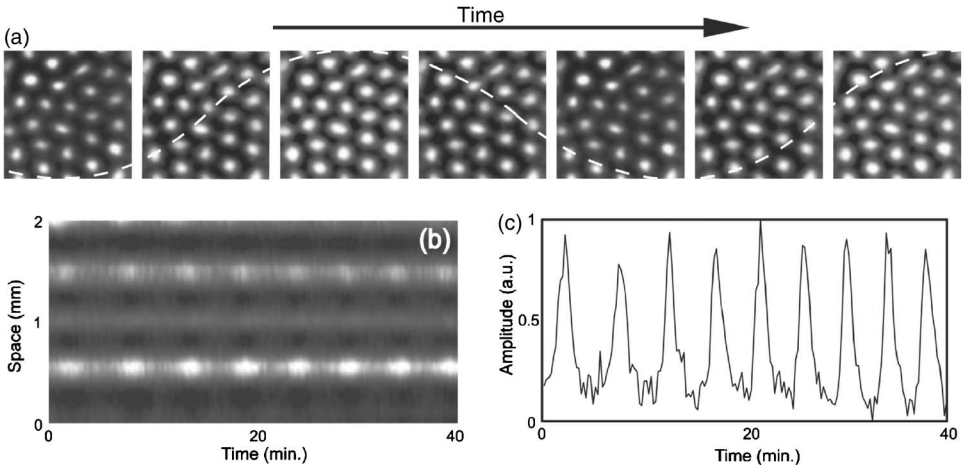

FIG. 13. In-phase oscillatory Turing patterns in the CDIMA reaction. (a) Series of snapshots of a region (2.5 mm×2.5 mm) with oscillating spots. The dashed sinusoidal line is drawn to help the eye identify the oscillations. (b) Space-time plot along a line in the system. (c) Local averaged concentration for an area involving about seven spots (Ref. 88).

of-phase oscillatory Turing patterns should also be possible,[40,87] but have yet not been found experimentally.

Another example of controlling patterns by temperature also comes from the BZ–AOT system, but here catalyzed by bathoferroin. In this system, dash-waves and segmented spirals were found at room temperature.[93,94] These remarkable waves were interpreted as resulting from interaction between trigger waves and Turing patterns that emerge out of an unstable state to which the system is locally switched by passage of the trigger wave. By increasing the temperature, we have found[39] a new class of waves that we refer to as "jumping waves."[95,96] This class of waves can be subdivided into three types: ordinary jumping waves (JW), bubble waves (BW), and rotating waves (RW).

Typical examples of JW are shown in Fig. 15(a), and their dynamical behavior is depicted in a space-time plot [Fig. 15(b)]. Each ordinary circular wave or target pattern propagates from its center until a new parallel arc suddenly appears a short distance ahead of the original wave. Then the parent wave vanishes and the new wave generates another parallel front a short distance ahead in the direction of propagation, and so on. Usually, the wavelength of a jump, λ_J, is between 100 and 250 μm, a distance comparable to the diffusion length $(D\tau)^{1/2}$.

Bubble waves and rotating waves propagate in the normal direction in the same manner as JW. The difference between JW, BW, and RW lies in the lateral propagation. An example of BW is shown in Figs. 15(c) and 15(d). BW usually evolve in time from JW or from conventional trigger waves (CW) via disruption or incomplete closure of wave fronts and are composed of discrete spots or "bubbles."

Rotating waves are another variant of jumping waves. RW typically occur at high temperatures (above 40 °C) and develop from JW. BW also can transform into RW, if the temperature is increased in the course of the experiment. These waves give the impression of wave rotation, a front circulating around the circumference of a circle. This sense comes from the very high normal wave velocity, v_n (60 μm/s for JW versus 12 μm/s for JW at 50 °C or even 3–5 μm/s at lower temperatures), and slow lateral propagation speed v_1 (15–40 μm/s at 50 °C). For RW, $v_n/v_1 > 1$ (or even $\gg 1$), while for JW, $v_n/v_1 \ll 1$. This lateral propagation is a form of phase wave. On occasion, a few successive rotating fronts of RW can be observed simultaneously, giving the impression of a rotating wheel.

A simple reaction-diffusion model first suggested by Purwins' group[97,98] and developed further in the Brandeis group[47,95] can describe both JW and segmented waves,

$$\partial u/\partial t = \alpha u - u^3 - k_3 v - k_4 w - k_1 + D_u \Delta u, \tag{3}$$

$$\partial v/\partial t = (u - v)/\varepsilon_1 + D_v \Delta v, \tag{4}$$

$$\partial w/\partial t = u - w + D_w \Delta w. \tag{5}$$

In the BZ–AOT system, u can be associated with the activator species $HBrO_2$, while v and w can be taken to represent the inhibitors, Br^- (water soluble) and Br_2 (oil soluble). However, it is not clear at the moment how temperature is linked to the parameters of the model.

VI. CONCLUSION

The systems we have described in this brief review give only a small glimpse into the rich world of pattern formation and the possibilities for its design and control in reaction-diffusion systems. There are many other methods to control patterns. Others, for example, have modified the boundary conditions by performing a reaction in a labyrinth of microchannels created by lithography,[99–101] or used an external electric field to control the wave velocity or the direction of wave propagation, and even to cause the wave to split.[102,103] It is also possible to modulate waves and patterns by inducing controllable convection in the medium.[104–110] Also, we have focused on systems in aqueous solution and in microemulsions, ignoring, for example, a considerable and impressive body of work on systems involving single crystals or membranes.[37]

As the reader will have discerned, the lines between design, control and "mere" investigation can often blur, and

Downloaded 27 Jun 2008 to 129.64.51.176. Redistribution subject to AIP license or copyright; see http://chaos.aip.org/chaos/copyright.jsp

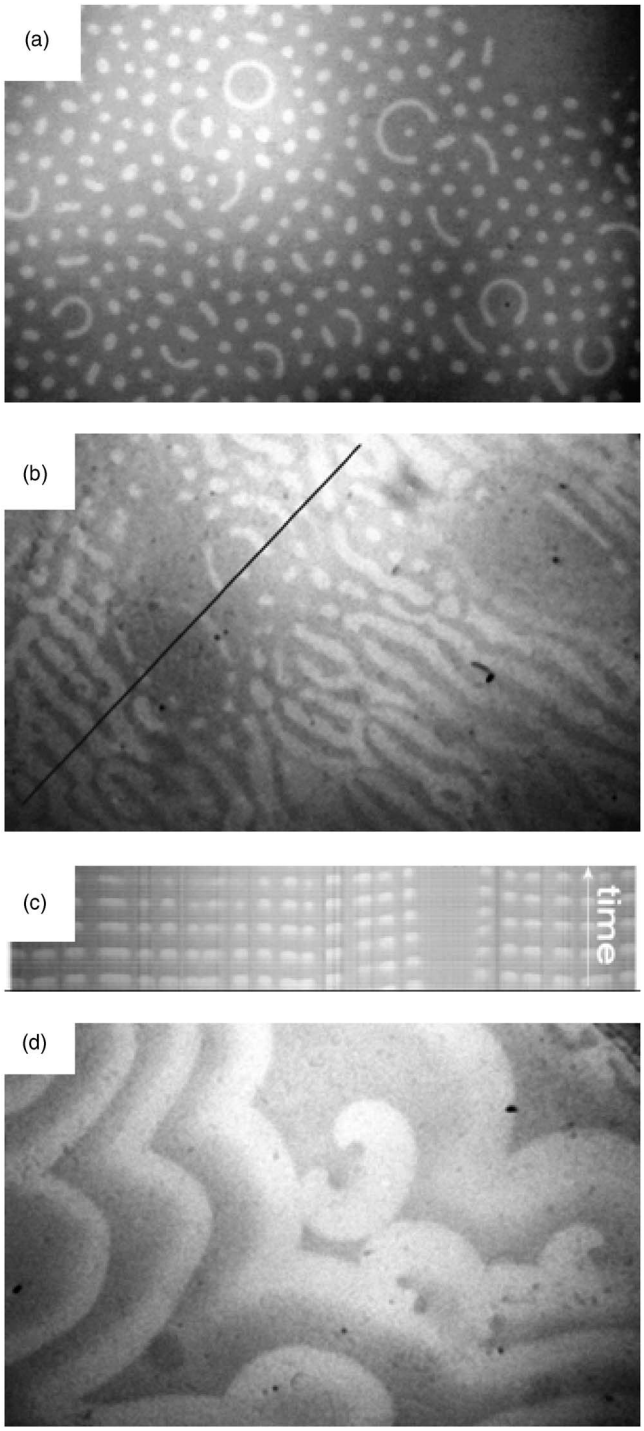

FIG. 14. Pattern formation in the $Ru(bpy)_3$-catalyzed BZ–AOT system at different temperatures. $[MA]_0=0.1$ M, $[H_2SO_4]_0=0.3$ M, $[NaBrO_3]_0=0.25$ M, $[Ru(bpy)_3]_0=0.004$ M, $\omega=10$, $\varphi_d=0.45$. (a) $T=25$ °C, Turing patterns, (b) $T=30$ °C, oscillatory Turing patterns; length of black diagonal line is 9 mm. (c) Space-time plot corresponding to line in (b); size is 9 mm×500 s, (d) $T=45$ °C, conventional waves and spiral waves. Frame size 11 mm×7 mm (Ref. 112).

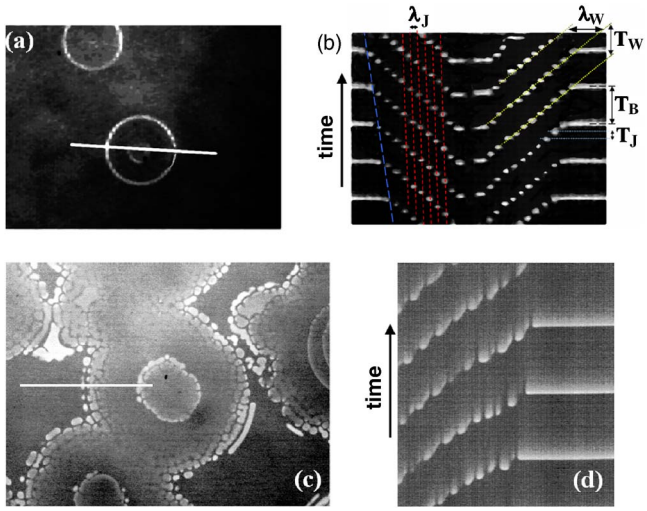

FIG. 15. (Color online) (a), (b) Jumping waves in the bathoferroin-catalyzed BZ–AOT system at 50 °C. $\omega=15$, $\varphi_d=0.6$, $[BrO_3^-]=0.18$, $[MA]=0.3$, $[H_2SO_4]=0.2$, [bathoferroin]=4.9 mM. Length of the white line in (a) is 4 mm. (b) Space-time plot along the line in (a) 4 mm×900 s. λ_J, wavelength of a jump; λ_W, wavelength of the wave; T_W, period for generating a new wave from a pacemaker; T_J, period of jumps of a single wave; $\lambda_J=T_J v_W$, and $\lambda_W=T_W v_W$, where v_W is the velocity of jumping waves; T_B is the period of bulk oscillations. (c), (d) Bubble waves in the bathoferroin-catalyzed BZ–AOT reaction $\omega=15$, $\varphi_d=0.6$, $[BrO_3^-]=0.213$ M, $[MA]=0.3$ M, $[H_2SO_4]=0.3$ M, [NaBr]=0.067 M, [Bathoferroin]=4.9 mM. $T=38$ °C. Size=(c) 7.9×5.9 mm^2 (d) 3.2 mm×600 s (Ref. 39).

how one characterizes a particular set of experiments may be quite subjective, perhaps depending more on one's viewpoint or on one's current level of understanding than on objective, contemporary reality. Nonetheless, it is clear that the richness of nonlinear phenomena in reaction-diffusion systems is a worthwhile area of study; much remains to be discovered, and the interplay between theory and experiment can only make that discovery process more effective, whether one thinks of it as design, control or something else. What makes the study of nonlinear phenomena so exciting, and often so surprising, is the existence of bifurcations. While a sufficient theoretical understanding of a system can enable one to predict in advance the location and the nature of the bifurcations, enabling a process of design and/or control, a less than complete picture (which is almost always what one has) can result in unexpected bifurcations turning up and converting what one thought was an exercise in design or control into one of discovery.

ACKNOWLEDGMENTS

This work was supported by the National Science Foundation under Grant No. CHE-0615507.

[1]W. C. Bray, J. Am. Chem. Soc. **43**, 1262 (1921).
[2]B. P. Belousov, in *Collection of Short Papers on Radiation Medicine* (Medgiz, Moscow, 1959), p. 145.
[3]A. M. Zhabotinsky, Russ. Acad. Sci. Bull. Phys. **157**, 392 (1964).
[4]V. Castets, E. Dulos, J. Boissonade, and P. De Kepper, Phys. Rev. Lett. **64**, 2953 (1990).
[5]J. M. Epstein, Complexity **4**, 41 (1999).
[6]P. De Kepper, I. R. Epstein, and K. Kustin, J. Am. Chem. Soc. **103**, 2133 (1981).
[7]J. Boissonade and P. De Kepper, J. Phys. Chem. **84**, 501 (1980).
[8]F. Sagués and I. R. Epstein, Dalton Trans. **7**, 1201 (2003).
[9]O. Decroly and A. Goldbeter, J. Theor. Biol. **124**, 219 (1987).
[10]C. E. Dateo, M. Orban, P. De Kepper, and I. R. Epstein, J. Am. Chem. Soc. **104**, 504 (1982).
[11]M. Alamgir, P. De Kepper, M. Orbán, and I. R. Epstein, J. Am. Chem. Soc. **105**, 2641 (1983).
[12]M. Alamgir and I. R. Epstein, J. Am. Chem. Soc. **105**, 2500 (1983).
[13]A. T. Winfree, Science **175**, 634 (1972).

Downloaded 27 Jun 2008 to 129.64.51.176. Redistribution subject to AIP license or copyright; see http://chaos.aip.org/chaos/copyright.jsp

[14]A. N. Zaikin and A. M. Zhabotinsky, Nature (London) **225**, 535 (1970).
[15]H. Yamada, T. Nakagaki, R. E. Baker, and P. K. Maini, J. Math. Biol. **54**, 745 (2007).
[16]S. Nagano, Dev., Growth Differ. **42**, 541 (2000).
[17]J. Lechleiter, S. Girard, E. Peralta, and D. Clapham, Science **252**, 123 (1991).
[18]J. D. Lechleiter and D. E. Clapham, J. Physiol. Paris **86**, 123 (1992).
[19]M. Orbán, C. Dateo, P. De Kepper, and I. R. Epstein, J. Am. Chem. Soc. **104**, 5911 (1982).
[20]M. Orbán, P. De Kepper, I. R. Epstein, and K. Kustin, Nature (London) **292**, 816 (1981).
[21]P. De Kepper, I. R. Epstein, K. Kustin, and M. Orbán, J. Phys. Chem. **86**, 170 (1982).
[22]Z. Noszticzius, W. Horsthemke, W. D. McCormick, H. L. Swinney, and W. Y. Tam, Nature (London) **329**, 619 (1987).
[23]V. Petrov, Q. Ouyang, and H. L. Swinney, Nature (London) **388**, 655 (1997).
[24]E. C. Edblom, M. Orbán, and I. R. Epstein, J. Am. Chem. Soc. **108**, 2826 (1986).
[25]D. Haim, G. Li, Q. Ouyang, W. D. McCormick, H. L. Swinney, A. Hagberg, and E. Meron, Phys. Rev. Lett. **77**, 190 (1996).
[26]K. J. Lee, W. D. McCormick, J. E. Pearson, and H. L. Swinney, Nature (London) **369**, 215 (1994).
[27]A. M. Turing, Philos. Trans. R. Soc. London, Ser. B **237**, 37 (1952).
[28]P. K. Maini, R. E. Baker, and C. M. Chuong, Science **314**, 1397 (2006).
[29]S. Sick, S. Reinker, J. Timmer, and T. Schlake, Science **314**, 1447 (2006).
[30]I. Lengyel and I. R. Epstein, Science **251**, 650 (1991).
[31]I. Lengyel, G. Rábai, and I. R. Epstein, J. Am. Chem. Soc. **112**, 9104 (1990).
[32]I. Lengyel and I. R. Epstein, Proc. Natl. Acad. Sci. U.S.A. **89**, 3977 (1992).
[33]T. K. De and A. Maitra, Adv. Colloid Interface Sci. **59**, 95 (1995).
[34]P. D. I. Fletcher, A. M. Howe, and B. H. Robinson, J. Chem. Soc., Faraday Trans. 1 **83**, 985 (1987).
[35]M. Kotlarchyk, S. H. Chen, and J. S. Huang, J. Phys. Chem. **86**, 3273 (1982).
[36]S. Ray, S. R. Bisal, and S. P. Moulik, J. Chem. Soc., Faraday Trans. **89**, 3277 (1993).
[37]A. S. Mikhailov and K. Showalter, Phys. Rep. **425**, 79 (2006).
[38]*Oscillations and Traveling Waves in Chemical Systems*, edited by R. J. Field and M. Burger (Wiley, New York, 1985).
[39]A. A. Cherkashin, V. K. Vanag, and I. R. Epstein (submitted).
[40]V. K. Vanag and I. R. Epstein, Phys. Rev. E **71**, 066212 (2005).
[41]V. K. Vanag and I. R. Epstein, Phys. Rev. E **67**, 066219 (2003).
[42]Q. Ouyang, Z. Noszticzius, and H. L. Swinney, J. Phys. Chem. **96**, 6773 (1992).
[43]I. Lengyel, G. Rábai, and I. R. Epstein, J. Am. Chem. Soc. **112**, 4606 (1990).
[44]L. F. Yang, M. Dolnik, A. M. Zhabotinsky, and I. R. Epstein, Chaos **16**, 037114 (2006).
[45]G. H. Gunaratne, Q. Ouyang, and H. L. Swinney, Phys. Rev. E **50**, 2802 (1994).
[46]A. Kaminaga, V. K. Vanag, and I. R. Epstein, Angew. Chem., Int. Ed. **45**, 3087 (2006).
[47]V. K. Vanag and I. R. Epstein, Chaos **17**, 037110 (2007).
[48]E. Mihaliuk, T. Sakurai, F. Chirila, and K. Showalter, Faraday Discuss. **120**, 383 (2001).
[49]T. Sakurai, E. Mihaliuk, F. Chirila, and K. Showalter, Science **296**, 2009 (2002).
[50]V. K. Vanag, L. Yang, M. Dolnik, A. M. Zhabotinsky, and I. R. Epstein, Nature (London) **406**, 389 (2000).
[51]V. K. Vanag, A. M. Zhabotinsky, and I. R. Epstein, J. Phys. Chem. A **104**, 11566 (2000).
[52]O. Lev, M. Sheintuch, L. M. Pisemen, and Ch. Yarnitzky, Nature (London) **336**, 458 (1988).
[53]A. Kaminaga, V. K. Vanag, and I. R. Epstein, Phys. Rev. Lett. **95**, 058302 (2005).
[54]V. K. Vanag and I. R. Epstein, Phys. Rev. Lett. **87**, 228301 (2001).
[55]M. Argentina, O. Rudzick, and M. G. Velarde, Chaos **14**, 777 (2004).
[56]C. Elphick, A. Hagberg, and E. Meron, Phys. Rev. Lett. **80**, 5007 (1998).
[57]C. Elphick, A. Hagberg, and E. Meron, Phys. Rev. E **59**, 5285 (1999).
[58]M. Hammele and W. Zimmermann, Phys. Rev. E **73**, 066211 (2006).
[59]R. M. Mantel and D. Barkley, Phys. Rev. E **54**, 4791 (1996).
[60]R. M. Mantel and D. Barkley, Physica D **149**, 107 (2001).
[61]N. Manz, V. A. Davydov, V. S. Zykov, and S. C. Müller, Phys. Rev. E **66**, 036207 (2002).
[62]B. Marts, A. Hagberg, E. Meron, and A. L. Lin, Phys. Rev. Lett. **93**, 108305 (2004).
[63]B. Marts, A. Hagberg, E. Meron, and A. L. Lin, Chaos **16**, 037113 (2006).
[64]H. Tokuda and T. Ohta, J. Phys. Soc. Jpn. **75**, 064005 (2006).
[65]E. P. Zemskov, K. Kassner, and S. C. Müller, Eur. Phys. J. B **34**, 285 (2003).
[66]H. Zhang, N. J. Wu, H. P. Ying, G. Hu, and B. Hu, J. Chem. Phys. **121**, 7276 (2004).
[67]H. Chaté, A. Pikovsky, and O. Rudzick, Physica D **131**, 17 (1999).
[68]J. Kim, J. Lee, and B. Kahng, Physica A **315**, 330 (2002).
[69]O. Rudzick and A. S. Mikhailov, Phys. Rev. Lett. **96**, 018302 (2006).
[70]K. I. Agladze, V. A. Davydov, and A. S. Mikhailov, JETP Lett. **45**, 767 (1987).
[71]V. A. Davydov, V. S. Zykov, and A. S. Mikhailov, Usp. Fiz. Nauk **161**, 45 (1991).
[72]V. S. Zykov, O. Steinbock, and S. C. Müller, Chaos **4**, 509 (1994).
[73]A. Schrader, M. Braune, and H. Engel, Phys. Rev. E **52**, 98 (1995).
[74]S. Kantrasiri, P. Jirakanjana, and O. U. Kheowan, Chem. Phys. Lett. **416**, 364 (2005).
[75]O. Steinbock, V. Zykov, and S. C. Müller, Nature (London) **366**, 322 (1993).
[76]V. K. Vanag, A. M. Zhabotinsky, and I. R. Epstein, Phys. Rev. Lett. **86**, 552 (2001).
[77]A. L. Lin, M. Bertram, K. Martinez, H. L. Swinney, A. Ardelea, and G. F. Carey, Phys. Rev. Lett. **84**, 4240 (2000).
[78]A. L. Lin, A. Hagberg, A. Ardelea, M. Bertram, H. L. Swinney, and E. Meron, Phys. Rev. E **62**, 3790 (2000).
[79]A. L. Lin, A. Hagberg, E. Meron, and H. L. Swinney, Phys. Rev. E **69**, 066217 (2004).
[80]S. Rudiger, D. G. Míguez, A. P. Muñuzuri, F. Sagués, and J. Casademunt, Phys. Rev. Lett. **90**, 128301 (2003).
[81]S. Rudiger, E. M. Nicola, J. Casademunt, and L. Kramer, Phys. Rep. **447**, 73 (2007).
[82]S. Rudiger, J. Casademunt, and L. Kramer, Phys. Rev. Lett. **99**, 028302 (2007).
[83]S. Zykov, V. S. Zykov, and V. Davydov, Europhys. Lett. **73**, 335 (2006).
[84]D. G. Míguez, M. Dolnik, A. P. Muñuzuri, and L. Kramer, Phys. Rev. Lett. **96**, 048304 (2006).
[85]D. G. Míguez, V. Pérez-Villar, and A. P. Muñuzuri, Phys. Rev. E **71**, 066217 (2005).
[86]A. De Wit, Adv. Chem. Phys. **109**, 435 (1999).
[87]A. Kaminaga, V. K. Vanag, and I. R. Epstein, J. Chem. Phys. **122**, 174706 (2005).
[88]D. G. Míguez, S. Alonso, A. P. Muñuzuri, and F. Sagués, Phys. Rev. Lett. **97**, 178301 (2006).
[89]L. Schlicht, J. H. Spilgies, F. Runge, S. Lipgens, S. Boye, D. Schubel, and G. Ilgenfritz, Biophys. Chem. **58**, 39 (1996).
[90]H. Kataoka, T. Eguchi, H. Masui, K. Miyakubo, H. Nakayama, and N. Nakamura, J. Phys. Chem. B **107**, 12542 (2003).
[91]Y. Feldman, N. Kozlovich, I. Nir, N. Garti, V. Archipov, and V. Fedotov, J. Phys. Chem. **100**, 3745 (1996).
[92]Y. Feldman, N. Kozlovich, I. Nir, and N. Garti, Phys. Rev. E **51**, 478 (1995).
[93]V. K. Vanag and I. R. Epstein, Phys. Rev. Lett. **90**, 098301 (2003).
[94]V. K. Vanag and I. R. Epstein, Proc. Natl. Acad. Sci. U.S.A. **100**, 14635 (2003).
[95]L. F. Yang, A. M. Zhabotinsky, and I. R. Epstein, Phys. Chem. Chem. Phys. **8**, 4647 (2006).
[96]I. P. Nagy, A. Keresztessy, and J. A. Pojman, J. Phys. Chem. **99**, 5385 (1995).
[97]M. Bode, A. W. Liehr, C. P. Schenk, and H.-G. Purwins, Physica D **161**, 45 (2002).
[98]C. P. Schenk, M. Or-Guil, M. Bode, and H.-G. Purwins, Phys. Rev. Lett. **78**, 3781 (1997).
[99]B. T. Ginn and O. Steinbock, Phys. Rev. E **72**, 046109 (2005).
[100]B. T. Ginn and O. Steinbock, Phys. Rev. Lett. **93**, 158301 (2004).
[101]L. Qiao, I. G. Kevrekidis, C. Punckt, and H. H. Rotermund, Phys. Rev. E **73**, 036219 (2006).
[102]H. Ševčiková and M. Marek, Physica D **9**, 140 (1983).
[103]H. Ševčiková, M. Marek, and S. C. Müller, Science **257**, 951 (1992).
[104]T. H. Solomon and I. Mezic, Nature (London) **425**, 376 (2003).

Downloaded 27 Jun 2008 to 129.64.51.176. Redistribution subject to AIP license or copyright; see http://chaos.aip.org/chaos/copyright.jsp

[105] M. S. Paoletti and T. H. Solomon, Phys. Rev. E **72**, 046204 (2005).
[106] M. S. Paoletti, C. R. Nugent, and T. H. Solomon, Phys. Rev. Lett. **96**, 124101 (2006).
[107] H. Miike, S. C. Müller, and B. Hess, Phys. Lett. A **141**, 25 (1989).
[108] S. Kai and H. Miike, Physica A **204**, 346 (1994).
[109] T. Sakurai, H. Miike, K. Okada, and S. C. Müller, J. Phys. Soc. Jpn. **72**, 2177 (2003).
[110] T. Sakurai, O. Inomoto, H. Miike, and S. Kai, J. Phys. Soc. Jpn. **73**, 485 (2004).
[111] A. Kaminaga, V. K. Vanag, and I. R. Epstein (unpublished).
[112] R. McIlwaine, V. K. Vanag, and I. R. Epstein (unpublished).

Downloaded 27 Jun 2008 to 129.64.51.176. Redistribution subject to AIP license or copyright; see http://chaos.aip.org/chaos/copyright.jsp